Northumbria Research Link

Citation: Davenport, Ian J., Sandells, Melody J. and Gurney, Robert J. The effects of scene heterogeneity on soil moisture retrieval from passive microwave data. Advances in Water Resources, 31 (11). pp. 1494-1502. ISSN 0309-1708

Published by: UNSPECIFIED

URL:

This version was downloaded from Northumbria Research Link: http://northumbria-test.eprints-hosting.org/id/eprint/55596/

Northumbria University has developed Northumbria Research Link (NRL) to enable users to access the University's research output. Copyright © and moral rights for items on NRL are retained by the individual author(s) and/or other copyright owners. Single copies of full items can be reproduced, displayed or performed, and given to third parties in any format or medium for personal research or study, educational, or not-for-profit purposes without prior permission or charge, provided the authors, title and full bibliographic details are given, as well as a hyperlink and/or URL to the original metadata page. The content must not be changed in any way. Full items must not be sold commercially in any format or medium without formal permission of the copyright holder. The full policy is available online: http://nrl.northumbria.ac.uk/policies.html

This document may differ from the final, published version of the research and has been made available online in accordance with publisher policies. To read and/or cite from the published version of the research, please visit the publisher's website (a subscription may be required.)

UniversityLibrary

Northumbria
University
NEWCASTLE

The effects of scene heterogeneity on soil moisture retrieval from passive microwave data

Ian J Davenport, Melody J Sandells, Robert J Gurney

Abstract

The Tau-Omega model of microwave emission from soil and vegetation layers is widely used to estimate soil moisture content from passive microwave observations. Its application to prospective satellite-based observations aggregating several thousand square kilometres requires understanding of the effects of scene heterogeneity. The effects of heterogeneity in soil surface roughness, soil moisture, water area and vegetation density on the retrieval of soil moisture from simulated single- and multi-angle observing systems were tested. Uncertainty in water area proved the most serious problem for both systems, causing errors of a few percent in soil moisture retrieval. Single-angle retrieval was largely unaffected by the other factors studied here. Multiple-angle retrievals errors around one percent arose from heterogeneity in either soil roughness or soil moisture. Errors of a few percent were caused by vegetation heterogeneity. A simple extension of the model vegetation representation was shown to reduce this error substantially for scenes containing a range of vegetation types.

Index terms: passive microwave soil moisture heterogeneity roughness vegetation water

I. INTRODUCTION

Until recently, two passive L-band microwave satellite-based instruments were planned with an appropriate configuration to measure soil moisture - the European Space Agency SMOS [1] and NASA Hydros[2]. These differ chiefly in the look angles at which data is acquired, Hydros would acquire data at 40 degrees from the vertical, whilst SMOS will acquire data at a range of angles between nadir and up to 60 degrees, depending on the target-swathe geometry. Whilst development on Hydros is suspended at the time of writing, it is likely that a single-angle spaceborne L-band passive microwave system will be deployed in the future, so in the work here we compare multiple- and single-angle microwave systems. The most widely used model to predict microwave emission from vegetated soil, and the one planned for use in the soil moisture retrieval algorithms for both systems, is the τ-ω model [3,4]. We have previously [5] shown how, for homogenous scenes, the retrieval of soil moisture is dependent on uncertainty in the variables used in the model to describe the scene, such as surface temperature, soil surface roughness, and the vegetation optical depth and single scattering albedo. The wavelength of L-band radiation and technical limitations on space-based antenna will enforce a mean spatial resolution of the order of 50 km. Any single observation will therefore almost invariably enclose a region of the Earth's surface with a range of each of the variables. In this paper we consider the effects of heterogeneity within a scene on a simple retrieval. In the case of a single-angle sensor, we will need to estimate some surface variables to retrieve soil moisture. We consider how best to incorporate estimates of heterogeneous variables, and question whether simple averages are adequate. For multiple-angle sensors, there may be enough information within the brightness temperature curves to accommodate some heterogeneity. In the absence of any existing observations covering the spatial extent covered by a satellite-based passive microwave instrument, and because of the impracticality of making reliable measurements over such a special extent, we have approached this problem by generating synthetic scenes, assuming that the Tau-Omega model is a realistic representation of microwave emission.

Past work in this area, conducted in the context of earlier passive microwave instruments operating at higher frequencies such as SSM/I and AMSR-E, has included studies of the effect of soil texture variability [6] and of heterogeneity in specific areas, using hydrologic models to estimate the extent of local surface feature variability [7,8]. In this paper we take a more general approach, examining the direct effects of variation in features of the soil surface and vegetation cover without limiting the range of variation to that expected at a particular site. In Section II we describe the model used for the variable retrieval, the methodology used to assess the effects of heterogeneity, and describe the four sources of heterogeneity to be investigated. We consider the effects of heterogeneity in soil surface roughness by simulating a surface with a plausible range of roughnesses. We examine the effects of soil moisture, analysing the retrieval error for a soil surface with a known mean moisture, but a range of actual values. We look at the effects of waterlogging, coastal water and inland water bodies by assuming a proportion of the scene is standing water. We evaluate both the effects of ignoring standing water, and incorporating a water fraction estimate into the retrieval. By varying vegetation optical depth within a scene, we examine the effects of retrieving soil moisture from a pixel which contains either a mixture of bare soil and vegetation, or a range of vegetation density. We discuss the problem posed by the non-linear effect of vegetation on observed

microwave radiation through a heterogeneous canopy, and present a means of reducing this effect by extending the representation of vegetation within the model. Section III presents the results of the analyses, in Section IV we discuss the results, and in Section V we draw together the conclusions to compare the relative effects of the sources, and consider what measures can be taken to reduce the effects of heterogeneity.

We do not present here any analysis of the effects of heterogeneity in temperature and vegetation single-scattering albedo. While any scene with a spatial extent of hundreds of square kilometres will exhibit some variability in these factors, this should have a negligible effect. Brightness temperature scales linearly with surface temperature, or more accurately the effective surface temperature, accounting for the optical depth of the surface, at any given look-angle when all other variables remain constant. Thus, the brightness temperature curve for a site comprised of a number of different soil temperature regions is identical to the brightness temperature curve for the mean temperature of the region. As long as the mean surface temperature is known, heterogeneity within it should contribute no error. Similarly, the dependence of brightness temperature on single-scattering albedo of vegetation within the model is also linear, and so whilst it is possible that in reality non-linearity may have an effect, this will be not evident from this modelling approach.

II. METHOD

A. Model description

As in our previous work, we use a simple radiative transfer formulation, the τ-ω model [3,4], to describe the emission of microwave radiation from the soil surface. In the τ-ω model, the brightness temperature, T_B, of a top layer (soil and vegetation) medium is the sum of three terms: the canopy attenuated soil emission, the direct vegetation emission and the vegetation emission reflected by the soil and attenuated by the canopy. A fourth term representing the soil-reflected and two way canopy-attenuated down-welling sky brightness temperature is sometimes implemented, but is considered negligible here. Hence, the brightness temperature can be expressed as:

$$\begin{aligned} T_B &= \varepsilon_{soil} \cdot T_{soil} \cdot e^{\frac{-\tau}{\cos\alpha}} + (1-\omega) \cdot T_{veg} \cdot (1 - e^{\frac{-\tau}{\cos\alpha}}) \\ &+ (1-\varepsilon_{soil}) \cdot (1-\omega) \cdot T_{veg} \cdot (1 - e^{\frac{-\tau}{\cos\alpha}}) \cdot e^{\frac{-\tau}{\cos\alpha}} \end{aligned} \quad (1)$$

where ε_{soil} is the soil emissivity, ω is the single scattering albedo within the canopy, τ is the optical depth of the canopy, α is the instrument look angle from nadir, T_{soil} is the soil temperature and T_{veg} is the vegetation temperature, which in this case we assume to be the same as the soil temperature.

The soil emissivity is calculated from the Fresnel equations, incorporating the dielectric permittivity of the soil which is derived from the Wang and Schmugge [9] model, assuming a soil texture of *SAND*=60%, *CLAY*=20%, incorporating the wilting point of soil [10] assuming a bulk density of 1.3 $g \cdot cm^{-3}$, and component relative dielectric permittivity of 3.2, 1 and 5.5 for bound water, air and soil particles respectively. The dielectric permittivity of water was derived by the modified version

of the Debye equation for the relative dielectric permittivity [11], the high frequency dielectric permittivity [12], the static dielectric permittivity of water as described by Klein and Swift [13] and the relaxation time of pure water [14].

B. Methodology

The effects of heterogeneity in soil surface roughness and soil moisture on retrieval accuracy are considered individually in the following sections. The brightness temperature curve produced by heterogeneity in each variable is simulated by combining brightness temperature curves produced by different values of the variable in the forward model. To simulate a multiple angle system, brightness temperature curves are generated at the angles 0,10,20,30,40,50 degrees from nadir at H and V polarisations, and for a single angle system, the brightness temperatures at 40 degrees from nadir are calculated at H and V polarisations. In each case, the retrieval then inverts the composite brightness temperature curves as described in [5] to recover the soil moisture content, vegetation optical depth and surface temperature, constraining the surface temperature to within 2K of the target, and using a single value of the heterogeneous variable. With observations at multiple angles, it is also often possible to retrieve a value for an additional unknown variable, so we also perform retrievals which attempt to retrieve a value for the heterogeneous variable. This becomes more difficult with a single-angle radiometer, which produces only two measurements, one at each of H and V polarisation. Since it is necessary to retrieve three variables, soil moisture content, vegetation optical depth and surface temperature, some constraint of the variables is necessary to produce solutions. It is commonly assumed that the surface temperature will be estimated to an accuracy of about 2 K for this purpose, so to simulate this we carry out a set of retrievals assuming a uniform range of surface temperatures within the 2K extent, and calculate error statistics based on these runs. Whereas a multiple-angle retrieval from a pair of brightness temperature curves will result in one unique best solution and a distinct error in each variable, a single-angle retrieval result will be based on a range of solutions based on the different surface temperature assumptions, and the range of possible solutions are included within the error statistics.

C. Heterogeneity in surface roughness

Soil roughness on the vertical scale of a centimetre can affect the microwave reflectivity, and consequently the emissivity of the surface, in a manner dependent on the look-angle [13]. This has an impact on the brightness temperature curves recorded by an observing system, and consequently the retrieval of the soil moisture, vegetation optical depth and surface temperature from these observations. Measurement of the soil surface roughness will in most cases be infeasible over the spatial scale of several hundreds of square kilometres covered by a satellite microwave radiometer (though a smaller scale technique is described in [14]). While this effect has a relatively minor influence on retrievals from a single-angle system in a homogeneous scene [5], accurate retrieval from a multiple-angle system relies upon allowing the algorithm to extract the roughness from the observations. This proves successful for a surface with a uniform roughness, however the soil surface over hundreds of square kilometres is likely to have a range of surface roughnesses.

The soil surface roughness modification to the τ-ω model suggested by Choudhury et al. [15] modifies the microwave reflectivity of the soil as per equation (2) …

$$R = R_0 e^{-h.\cos^2 \alpha} \tag{2}$$

where R_0 is the reflectivity of flat soil, α is the look angle, h is the roughness factor given by

$$h = 4\sigma^2 \left(\frac{2\pi}{\lambda} \right)^2 \tag{3}$$

where σ is the standard deviation of the surface elevation and λ is the microwave wavelength. h = 0.0 for flat, 0.3 at maximum, and typically on average 0.1. For the 21 cm radiometer, the maximum 0.3 indicates a surface with σ = 9 mm, which is slightly lower than some freshly cultivated sites. Field measurements showed[16] that a field recently harrowed with a rotary cultivator gave a surface with a peak-trough range of 30 mm, and a standard deviation of 9.8 mm over a 1 m distance, and a recently-ploughed site with a peak-rough range of about 50 mm had an elevation standard deviation of 15.7 mm over 1 m. However, since these sites were cultivated only a few days before measurement, and would flatten quickly with weather conditions, the maximum of 0.3 was considered appropriate for this study.

A number of test scenarios were generated by combining soil with a range of moisture between 0.10 and 0.40 m^3m^{-3} with vegetation with a range of vegetation optical depths between 0.0 and 0.6. A soil surface with equal proportions of roughnesses 0.0, 0.1, 0.2, 0.3, was simulated by taking the mean brightness temperature curves over the four roughness values for each scenario. We then attempted to retrieve soil moisture, vegetation optical depth and surface temperature from each of the curve pairs. The effect of independent surface temperature information was simulated by fitting the curves whilst restricting the retrieved surface temperature to fall within 2 K of the input value, which was kept at 293 K. For the single-angle system the retrieval assumed a mean value of soil roughness of 0.15. For the multiple-angle retrievals two techniques were attempted; firstly assuming a mean value of soil roughness and secondly, to use the greater number of observations in the multiple-angle data, retrieving the soil roughness as a fourth variable.

D. Variation in soil moisture

Soil moisture will not be uniform over the hundreds of square kilometres covered by a satellite radiometer footprint. If a fraction of the target area has significantly different moisture content, or there is substantial variation in the area, we need to know how this affects its retrieval accuracy. These variations can be caused naturally by any number of mechanisms such as flooding or non-uniform precipitation or drainage, or man-made, such as extensive areas of irrigation in otherwise arid areas.

The six scenarios generated by combining vegetation optical depths 0.0, 0.2, 0.6 with soil moisture 0.1 and 0.4 m^3m^{-3} were analysed here. To simulate areas with a range of soil moisture with a known mean, brightness temperature curves were generated around each scenario by taking the mean of curves with a spread in the soil moisture,

as indicated in Table 1. Intermediate spread extents were also similarly devised between these for the same two soil moisture values. Retrievals then attempted to recover the soil moisture, vegetation optical depth and surface temperature from the simulated observations.

E. The presence of open water

The different microwave behaviour of open water means that the presence of waterlogged areas, water bodies, rivers and coasts within a scene will alter the microwave radiation received from a scene, and this, if uncorrected in the retrieval, will cause errors in the retrieved soil moisture. We analyse two possible cases; firstly the presence of water in a scene when we assume that there is no open water, and secondly where we have a non-exact estimate of open water fraction within a scene.

The microwave emission of water is calculated assuming that the surface is flat and the water fresh [15], and its brightness temperature curve is then combined with that of each of the six scenarios, covering vegetation optical depth 0.0, 0.2, 0.6 and soil moisture 0.1 and 0.4 m^3m^{-3}, to create composite curves for scenarios in which water covers a variable amount of the scene. Retrievals then attempted to recover the soil moisture, vegetation optical depth and surface temperature from the simulated observations, using the assumption that the scene does not have any water coverage.

Additionally, in order to determine how much of the effect of water in a scene can be compensated for by prior information on water cover, we generated scenes for each soil moisture and vegetation optical depth scenario which included a known proportion of open water, and attempted to retrieve the soil moisture with a retrieval which assumed a water fraction with an error. So, for instance, where a set of brightness temperature curves for a certain case corresponded to 32% of the pixel being covered with water, we set up retrievals to account for the effect of the water based on the assumptions that water covered (i) 31.8% and (ii) 32.2% of the scene, to measure the effect of a 0.2% error in water fraction estimation. The same six soil moisture and vegetation optical depth scenarios described above are employed for this analysis, and water is modelled in the forward and inverse stages as flat fresh open water.

F. Heterogeneity in vegetation density

All vegetation types will show significant variation in density and therefore in microwave optical depth on the spatial scale of hundreds of square kilometres. Whilst we may be able to make an estimate of the mean vegetation cover for a given area, vegetation optical depth will rarely be uniform over this scale. Since a major effect of the vegetation layer is to exponentially attenuate the radiation emitted by the soil surface, brightness temperature curves will not scale linearly with τ. Therefore, a pixel containing areas with a range of vegetation optical depths will not have the same brightness temperature curve as a pixel with a single uniform optical depth with the same mean.

In reality, vegetation cover will often be complex, with multiple layers of overlapping vegetation types with differing optical depth and albedo characteristics, for example trees, grass and undergrowth. It would clearly be very difficult to create a model

which accommodated such variation, with variables for the characteristics and extent of overlap of each layer, so we test here two simpler cases which assume that any one area has only one vegetation cover type. Firstly, we simulate an area which is a combination of bare soil and consistent vegetation. Secondly, we simulate a more mixed area with vegetation types with seven different optical depths.

For the case where we consider a scene containing both bare soil and vegetation, the soil moisture and surface temperature are assumed constant across the scene. We consider six simple surface scenarios comprising the combinations of soil moisture θ=0.1 and 0.4 m^3m^{-3}, and vegetation optical depth τ =0.0, 0.2, 0.6. Test brightness temperature curves were devised by combining the curves for the two vegetated scenarios (τ = 0.2, 0.6) individually with the bare soil scenario (τ =0.0) for each of the soil moisture values θ=0.1 and 0.4 m^3m^{-3}. Scenes are synthesised which contain a range of areas of bare soil and vegetation by creating brightness temperature curves with different ratios of the vegetated and bare soil curves. We then attempt to retrieve the soil moisture, vegetation optical depth and surface temperature from the brightness temperature curves, constraining the surface temperature to within a 2 K range to simulate assimilation of surface temperature information. A similar analysis was carried out by Van de Griend et al [22] to simulate the effect of heterogeneity on retrievals from the SMOS instrument, however we also here propose and test two extensions to the retrieval model in an attempt to reduce the expected effect of the non-linear vegetation optical depth mixing.

Since our representation of the multiple-angle dual-polarisation instrument yields eleven independent measurements simultaneously, it is possible that information about vegetation optical depth heterogeneity could be extracted from these measurements. We tested whether this is the case, and how much a more complex vegetation representation improves the soil moisture retrieval. Our enhancement of the inverse model allows the retrieval algorithm to assume that the scene is composed of two different cover types. To add just one more variable to the analysis, we devised a retrieval which assumed that the second vegetation type had an optical depth of zero, i.e. the scene is a linear mix of an unknown vegetation type, and bare soil. In this case, all the retrieval has to find in addition to the previous retrievals is the ratio between the areas of bare soil and covered soil. This is represented by equation (4), where p represents the proportion of the scene covered with vegetation.

$$T_B = p \cdot \begin{pmatrix} \varepsilon_{soil} \cdot T_{soil} \cdot e^{\frac{-\tau}{\cos\alpha}} + (1-\omega) \cdot T_{veg} \cdot (1 - e^{\frac{-\tau}{\cos\alpha}}) \\ + (1-\varepsilon_{soil}) \cdot (1-\omega) \cdot T_{veg} \cdot (1 - e^{\frac{-\tau}{\cos\alpha}}) \cdot e^{\frac{-\tau}{\cos\alpha}} \end{pmatrix} + (1-p) \cdot \varepsilon_{soil} \cdot T_{soil} \qquad (4)$$

A further refinement is to allow a second vegetation cover area, so that the scene is a mix of two vegetation types. This requires the retrieval algorithm to estimate three variables pertaining to the vegetation optical depth – two optical depths, and the ratio between the areas covered by them. This is represented by equation (5), where p now represents the proportion of the scene covered with the first optical depth τ_1, and the rest of the scene is covered by vegetation with the second optical depth τ_2.

$$T_B = p \cdot \left(\begin{array}{l} \varepsilon_{soil} \cdot T_{soil} \cdot e^{\frac{-\tau_1}{\cos\alpha}} + (1-\omega) \cdot T_{veg} \cdot (1 - e^{\frac{-\tau_1}{\cos\alpha}}) \\ + (1-\varepsilon_{soil}) \cdot (1-\omega) \cdot T_{veg} \cdot (1 - e^{\frac{-\tau_1}{\cos\alpha}}) \cdot e^{\frac{-\tau_1}{\cos\alpha}} \end{array} \right) + (1-p) \cdot \left(\begin{array}{l} \varepsilon_{soil} \cdot T_{soil} \cdot e^{\frac{-\tau_2}{\cos\alpha}} + (1-\omega) \cdot T_{veg} \cdot (1 - e^{\frac{-\tau_2}{\cos\alpha}}) \\ + (1-\varepsilon_{soil}) \cdot (1-\omega) \cdot T_{veg} \cdot (1 - e^{\frac{-\tau_2}{\cos\alpha}}) \cdot e^{\frac{-\tau_2}{\cos\alpha}} \end{array} \right) \quad (5)$$

Clearly, both models should cope with the area which is a simple mix of bare soil and vegetated soil, however we also tested how such a retrieval performs with a mixture of more vegetation optical depths, in the hope that allowing the retrieval to incorporate some simple vegetation heterogeneity would improve its performance in more complicated scenarios.

To test the ability of a two- or three-variable τ retrieval as above to compensate for optical depth heterogeneity, we generated a test data set of 200 composite areas, 100 areas with soil moisture 0.1 m^3m^{-3} and 100 areas with soil moisture 0.4 m^3m^{-3}. Each area is a composite of the seven vegetation optical depths 0.0, 0.1, 0.2, 0.3, 0.4, 0.5, and 0.6, in randomly-selected proportions. The brightness temperature curves are thus weighted averages of the seven brightness curves, with the weights determined randomly. We then attempted to retrieve the soil moisture from each of these test HV curve pairs using the three possible vegetation optical depth representations – the basic single-τ inverse model, the two-variable model in equation (4) which retrieves τ and p, and the three-variable model in equation (5) which retrieves τ_1, τ_2 and p. We also tested the effect of this seven-τ cover on the single-angle retrieval, because there are insufficient measurements to retrieve additional variables.

III. RESULTS

A. Heterogeneity in surface roughness

Figures 1-3 show the effect of roughness heterogeneity on soil moisture retrieval errors. Figure 1 shows the effect of assuming a mean value of soil roughness using a single-angle system, compared to the homogenous retrievals in which the soil roughness is known as 0.0. Figure 2 shows the effect of assuming a mean value of soil roughness using a six-angle system. Figure 3 shows the effect of attempting to retrieve soil roughness from the six-angle data. Table 2 gives the statistics over all soil moisture and vegetation optical depth scenarios for each system and retrieval methodology.

1) Single-angle system

The retrieval errors are notably only marginally higher than the homogeneous retrieval error. The maximum error corresponds to the high soil moisture, high vegetation optical depth scenario.

2) Six-angle system

Using the roughness assumption of the mean value 0.15 for the six-angle system yields a mean error over all scenarios of 0.007 m^3m^{-3}, with a worst case 0.021 m^3m^{-3} for the high moisture and 0.4 vegetation optical depth scenario. In the homogeneous case, there is sufficient information in the brightness temperature curves to derive these variables exactly.

Allowing the retrieval from the six-angle data to find the best value of roughness improves the retrieval of the soil moisture to a mean error of 0.003 m^3m^{-3}, with a worst case of 0.014 m^3m^{-3}, where the soil moisture is maximum, and the optical depth 0.2. The value of soil roughness *h* retrieved by the algorithm has a mean of 0.139 with a standard deviation of 0.003, significantly and consistently lower than the mean of the constituent areas of 0.15.

B. Variation in soil moisture

The error in retrieving mean soil moisture from areas with a range of soil moisture values is shown in Figure 4. The single-angle retrieval errors increase very little as the spread increases, increasing in the worst case by 0.005 m^3m^{-3}. For the six-angle system, a spread in soil moisture of +/- 0.10 m^3m^{-3} results in a worst case error of 0.017 m^3m^{-3}.

C. The presence of open water

The effect of ignoring open water in soil moisture retrieval is shown in Figure 5.

The single-angle system errors shown in Figure 5(a) are higher than the six angle errors shown in Figure 5(b) because of the lower amount of information in only two measurements. Also, the single-angle errors increase more quickly than the six-angle errors, and exceed 0.04 m^3m^{-3} in the worst scenario (low soil moisture, high

vegetation cover) for only 2% water area, rising to 0.10 m^3m^{-3} when about 4% of the scene is covered with water.

For the six-angle system, Figure 5(b), the worst scenario (low soil moisture, high vegetation cover) error exceeds 0.04 m^3m^{-3} when about 4% of the scene is covered with water. This is equivalent to a 2 km width of water along one edge of 50 km x 50 km square pixel, or a 10 km x 10 km water body within the same pixel. It is notable, however, that in some cases even a 1% water area within the scene can give rise to a 0.01 m^3m^{-3} error in soil moisture retrieval. This could correspond to a 500 m wide river passing through the scene, a 500 m error in delineating a land-sea boundary for a coastal pixel, or a 5 km x 5 km water body.

In Figure 6 we show a plot of the soil moisture single-angle retrieval error for the case where we account for the effect of water, which shows an error up to 0.10 m^3m^{-3} if we have a 0.2% water fraction error, and the water fraction is 50%. An error in water fraction estimation of 0.5% causes the same soil moisture retrieval error, but both retrievals are constrained by physical considerations, since we limit soil moisture to between 0.00 and 0.50 m^3m^{-3}. When the scenario giving rise to the maximum error reaches a constraint, as happens in both Figures 6(a) and 6(b) around 50% water cover, the maximum absolute error curve causes the odd discontinuities seen in the plots. For the single-angle error cases, the mean soil moisture retrieval error for a 50% water pixel is 0.24 and 0.25 m^3m^{-3} for the 0.2 and 0.5% water fraction errors respectively.

In Figure 7 we show the same analysis for the six-angle system. For a scene which is 50% covered with open water, which might be a coastal zone scene, a 0.2% error in estimating the water fraction gives rise to a maximum error over all scenarios of 0.005 m^3m^{-3}, whereas an error as high as 0.5% in water fraction can give rise to a maximum error of 0.013 m^3m^{-3}.

D. Heterogeneity in vegetation density

Figure 8 shows the error in retrieved soil moisture for a pixel that is a mix of bare soil and soil covered with vegetation. The single-angle system is largely unaffected, with its mean soil moisture retrieval around the 0.01 m^3m^{-3} level dictated by the surface temperature constraint of 2 K. The error is close to a linear mixture of the errors of the extreme cases, with the maximum absolute error in the mixed area only exceeding the completely vegetated case by 0.002 m^3m^{-3} in the regime where about 5% of the pixel is bare. The single-angle system sensitivity to the simple scene, the bare soil/vegetated scene and the seven optical depth scenes is shown in Table 3. The mean error is largely unaffected by vegetation heterogeneity, and is marginal compared to the error induced by the estimation in surface temperature.

The six-angle system is significantly affected by the mixture, however, because the shape of the brightness temperature curve does not correspond to a single-tau scenario, and so the other variables are distorted to match the composite curve. Consequently, any scene containing other than one uniform vegetation optical depth will be misinterpreted.

The results of extending the inverse model to account for heterogeneous vegetation as described by equations (4) and (5) are given in Table 4. This indicates for example that the more complex representation of optical depth dramatically reduces the mean error caused by heterogeneity from 0.023 m^3m^{-3} in the single optical depth assumption to 0.001 m^3m^{-3} for the three-variable representation.

IV. DISCUSSION

A. Heterogeneity in surface roughness

The effect of soil surface roughness heterogeneity on single-angle retrievals is negligible compared to the effect of surface temperature constraint, since at a single angle, the change in the brightness temperature is relatively small. The strong angular dependence of surface roughness on emissivity [5] does cause larger errors for the six-angle system, however, when forced to assume a value of roughness. As the retrieval attempts to fit observations between nadir and 50º off-nadir, the mistaken assumption of the roughness forces the other model variables to be perturbed to make a better fit to the model. Since the six-angle system, when allowed to retrieve roughness, yields a roughness value lower than the mean of the constituent areas, the combined effect of a number of areas with different roughnesses is not linear, as can also been seen from equations (2) and (3), and care needs to be taken if assimilating surface roughness data of a heterogeneous target area into a retrieval scheme.

B. Variation in soil moisture

The effect of within-scene variation in soil moisture has a small effect on retrievals from the single-angle data, whilst the effect is more marked in multiple-angle retrievals for what is a plausible spread in soil moisture over hundreds of square

kilometres. This can be seen from the relationship between soil moisture and dielectric permittivity, which is linear for small changes in soil moisture, but shows some deviation from the linear over a greater range, the extent of which depends on which of the many published relationships is used. Whilst there is some variation between the relationships, each of them increases in slope when soil dielectric permittivity is plotted against soil moisture, and this increase in slope is responsible for the integrating error. Because of the uncertainty in this relationship, the size of this error may not be exact, but the commonality between models suggests that it is approximately right.

C. The presence of open water

The effects of including fairly small areas of water within a detector field of view have a serious impact on retrievals both when the effect of water is ignored, and when it is accounted for inexactly. The size of soil moisture retrieval error caused by only a small error in water fraction estimation of 0.2 %, which would amount to a tidal movement of 100 m in a 50 km wide scene, suggests that inaccuracy in water fraction estimation could cause significant problems for soil moisture retrievals from single- and multiple-angle microwave radiometers. This is due to the very different emissivities of water and soil. This is a relatively difficult problem, as while some of the other sources of contamination analysed here distort the brightness temperature curves, and therefore may be at least identified, if not quantified, the presence of more or less open water than expected merely makes the curves represent the scene as if it is wetter or drier than it in fact is. The only way to address this problem is to improve our estimation of the open water content of the scene.

D. Heterogeneity in vegetation density

For the single-angle system, vegetation mixture does not seem to cause significant retrieval problems. In the case where a pixel contains two or more levels of vegetation cover, or is partially vegetated and partially bare, the soil moisture retrieval error is simply the weighted average of the errors for the extreme cases, proportional to the areas covered.

The accuracy of retrievals from the six-angle system is significantly diminished if a single vegetation optical depth is assumed, as previously established by Van de Griend et al[22], since the simple representation of vegetation in the model does not allow brightness temperature curves of the shape seen with multiple vegetation types to be generated. Consequently the curves generated by the fit are poor matches generated by changing the other model variables, including soil moisture. An extension of the vegetation representation in the model can be used to incorporate vegetation optical depth variability, and substantially reduce this effect.

V. CONCLUSIONS

Within-pixel heterogeneity is likely to be an issue in most retrievals from L-band passive microwave radiometers, but the size of the problem has not been investigated before, other than empirically. This study has investigated this issue by attempting to retrieve soil moisture from idealised heterogeneous cases. The relative sizes of errors caused by the sources of error considered here are summarised in Table 5.

Soil roughness is possibly the most difficult of the parameters studied here to estimate on the required scale. While estimates might be made for large homogeneous areas, the variation caused by historic and current water flow, rainfall and different levels of vegetation growth and civilisation makes large scale accurate estimates unlikely. Fortunately, heterogeneity in soil roughness seems to have only a small effect on soil moisture retrieval from single-angle data. It affects multiple-angle data more seriously, but this error can be reduced by retrieving a representative value of soil roughness from the data. While the largest effect seen in the retrievals here is significant, the mean error is only 0.003 m^3m^{-3}.

Reasonable spreads in soil moisture yield a similar magnitude of results, though uncertainty in the relationship between soil permittivity and moisture content makes the exact level unclear. It is not obvious how this can be mitigated. Most areas with a significant level of soil moisture will also have a significant range, particularly on the spatial scale of hundreds of square kilometres. Possibly modifications to the emission model could be made, to represent a heterogeneous emitting area, but it is unclear how retrievals from such a model might work.

More seriously, small, unknown areas of water in the scene can potentially have a considerable effect on retrieval, with even small errors in water fraction able to cause substantial errors amounting to a significant fraction of the total SMOS/HYDROS instrumental error targets of 0.04 m^3m^{-3}. Clearly this effect needs accounting for in a system error budget, using auxiliary data. This is likely to be most difficult in areas of ephemeral surface water and flooding. Even accounting for the effect of static water bodies may well cause problems for retrievals, as precise and accurate global water body area information is surprisingly difficult to locate. Classified remote sensing data such the University of Maryland Database [18], or Europe's CORINE [19][20] are too coarse to provide accurate estimates of water cover area, and will not incorporate dynamic water events such as tides and floods . Vector river databases such as the drainage feature in ESRI's 'Digital Chart of the World' [21] dataset generally do not include information on river width, forcing us to generate water fractions based on river width estimates. This suggests to us that auxiliary water cover data of higher temporal and spatial resolution than is presently available will be necessary to accurately retrieve soil moisture from remotely-sensed L-band passive microwave data.

The effect of vegetation optical depth heterogeneity would also appear to be significant, but in this case is manageable. Since the major effect of vegetation in the τ-ω model is to obstruct the target surface by exponential attenuation, it should not be a surprise that a simplistic implied additive representation of vegetation as used in the basic model proves inadequate. However, a minor modification to the model, representing vegetation as a weighted average of bare soil and vegetation,

significantly reduces the error induced by heterogeneity, and this should be considered for algorithms intending to retrieve soil moisture from heterogeneous areas using multiple-angle observations. Also, whilst this technique may prove useful in scenes with planar heterogeneity in vegetation cover, we have not, as indicated earlier, here extended the heterogeneity vertically, and considered scenes which have multiple simultaneous and overlapping vegetation layers, such as wooded areas with understories of grass and undergrowth. Clearly there are far more combinations of these types of scenes than we could consider here, and whilst we suspect that the vegetation type with the longest optical depth would tend to dominate, this area may warrant further study.

ACKNOWLEDGMENT

The authors are grateful for the advice of D. Pearson (U.K. Meteorological Office), and L. Simmonds (Department of Soil Science at Reading University, U.K.).

REFERENCES

[1] Entekhabi, D., Njoku, E.G., Houser, P., Spencer, M., Doiron, T., Kim, Y., Smith, J., Girard, R.; Belair, S.; Crow, W.; Jackson, T.J.; Kerr, Y.H.; Kimball, J.S.; Koster, R.; McDonald, K.C.; O'Neill, P.E.; Pultz, T.; Running, S.W.; Jiancheng Shi; Wood, E.; van Zyl, J., 2004, The Hydrosphere State (Hydros) Satellite mission: an Earth system pathfinder for global mapping of soil moisture and land freeze/thaw, IEEE Transactions on Geoscience and Remote Sensing, **42** (10), 2184- 2195

[2] Kerr, Y.H., Waldteufel, P., Wigneron, J.-P., Martinuzzi, J.-M., Font, J., Berger, M., 2001, Soil Moisture Retrieval from Space: The Soil Moisture and Ocean Salinity (SMOS) Mission, IEEE Transactions on Geoscience and Remote Sensing, **39** (8), 1729-1735

[3] Mo, T., Choudhury, B.J., Schmugge, T.J., Jackson, T.J., 1982, A model for microwave emission from vegetation-covered fields, Journal of Hydrology, **184**, 101-129.

[4] Brunfeldt, D.R., Ulaby, F.T., 1984, Measured microwave emission and scattering in vegetation canopies, IEEE Transactions on Geoscience and Remote Sensing, **22** (6), 520-524.

[5] Davenport, I.J., Fernandez-Galvez, J., Gurney, R.J., 2005, A sensitivity analysis of soil moisture retrieval from the Tau-Omega microwave emission model, IEEE Transactions on Geoscience and Remote Sensing **43** (6), 1304-1316.

[6] Galantowicz, J.F., Entekhabit, D, Njoku, E., 2000, Estimation of Soil-Type Heterogeneity Effects in the Retrieval of Soil Moisture from Radiobrightness, IEEE Transactions on Geoscience and Remote Sensing, **38** (1) 312-316

[7] Crow, W.T., Drusch, M., Wood, E.F., 2001, An Observation System Simulation Experiment for the Impact of Land Surface Heterogeneity on AMSR-E Soil Moisture Retrieval, IEEE Transactions on Geoscience and Remote Sensing, **39** (8), 1622-1631

[8] Lakshmi, V., Wood, E.F., Choudhury, B.J., 1997, Investigation of effect of heterogeneities in vegetation and rainfall on simulated SSM/I brightness temperatures, International Journal of Remote Sensing, **18** (13), 2763-2784

[9] Wang, J.R., Schmugge, T.J., 1980, An empirical model for the complex dielectric permittivity of soil as a function of water content, IEEE Transactions on Geoscience and Remote Sensing, **18**, 288-295.

[10] Schmugge, T., Wilheit, T., Webster, W., Jr, Gloerson, P., 1976, "Remote sensing of soil moisture with microwave radiometers – II", National Aeronautics and Space Administration, NASA TN D-8321.

[11] Ulaby, F.T., Morre, R.K., Fung, A.K., 1986, "Microwave Remote Sensing, Active and Passive, Vol. III: From Theory to Applications", Artech House, Massachusetts.

[12] Lane, J.A., Saxton, J.A., 1952, Dielectric dispersion in pure polar liquids at very high radio-frequencies, measurements on water, methyl and ethyl alcohols, Proceedings of the Royal Society, **A213**, 400-408.

[13] Klein, L.A., Swift, C.T., 1977, An improved model for the dielectric constant of sea water at microwave frequencies, IEEE Transactions on Antennas and Propagation, **AP-25**, 104-111.

[14] Stogryn, A., 1970, The brightness temperature of a vertically structured medium, Radio Science, **5 (**12), 1397-1406.

[15] Choudhury, B. J., Schmugge, T. J., Chang, A., Newton, R. W., 1979, Effect of Surface Roughness on the Microwave Emission From Soils, Journal of Geographical Research, **18** (C9), 5699-5706

[16] Davenport, I.J., Holden, N., Gurney, R.J., 2004, Characterizing errors in airborne laser altimetry data to extract soil roughness, IEEE Transactions on Geoscience and Remote Sensing, **42** (10), 2130-2141

[17] Matzler, C. 1994, Passive Microwave Signatures of Landscapes in Winter. Meteorology and Atmospheric Physics, **54**, 241-260.

[18] Hansen, M.C., Defries, R.S., Townshend J.R.G., Sohlberg, R., 2000, Global land cover classification at 1km spatial resolution using a classification tree approach, International Journal of Remote Sensing, **21** (6-7) 1331-1364

[19] http://dataservice.eea.eu.int/dataservice/

[20] Brown, N., Gerard, F., Fuller, R. , 2002, Mapping of land use classes within the CORINE Land Cover Map of Great Britain, Cartographic Journal, **39** (1) 5-14

[21] http://www.lib.ncsu.edu/stacks/gis/esridm/2004/help/world/rivers.sdc.htm

[22] Van de Griend, A.A., Wigneron, J-P., Waldteufel, P., 2003, Consequences of surface heterogeneity for parameter retrieval from 1.4-GHz multiangle SMOS observations, IEEE Transactions on Geoscience and Remote Sensing, **41** (4), 803-811.

Mean soil moisture θ ($m^3 \cdot m^{-3}$)	Soil moisture θ heterogeneity, maximum deviation from mean…		
	0.10 $m^3 \cdot m^{-3}$	0.05 $m^3 \cdot m^{-3}$	0.01 $m^3 \cdot m^{-3}$
	θ values used for composite brightness temperature curve ($m^3 \cdot m^{-3}$)		
0.1	0.0, 0.05, 0.10, 0.15, 0.20	0.05, 0.075, 0.10, 0.125, 0.15	0.09, 0.095, 0.10, 0.105, 0.11
0.4	0.30, 0.35, 0.40, 0.45, 0.50	0.35, 0.375, 0.40, 0.425, 0.45	0.39, 0.395, 0.40, 0.405, 0.41

Table 1. Example heterogeneous soil moisture scenarios – the values of soil moisture content used to represent moisture heterogeneity.

Source data	Single-angle	Six-angle	
Retrieval system	Assume h=0.15	Assume h=0.15	Retrieve h
Mean absolute error ($m^3 \cdot m^{-3}$)	0.011	0.007	0.003
Maximum error ($m^3 \cdot m^{-3}$)	0.049	0.021	0.014

Table 2. Soil moisture retrieval errors (mean and maximum) from an area heterogeneous in soil roughness h.

Number of τ's in test data	Soil moisture retrieval error (mean / maximum) ($m^3 m^{-3}$)
1	0.010 / 0.042
2	0.010 / 0.046
7	0.011 / 0.033

Table 3. Soil moisture retrieval from τ-homogeneous and heterogeneous regions, using a single-angle system.

	Retrieval assumption about τ		
	Single τ	Vegetation / bare soil model, eq. (2)	Two vegetation optical depths model, eq. (3)
Number of τ's in test data	Soil moisture retrieval error (mean / maximum) ($m^3 m^{-3}$)		
1	0 / 0	0 / 0	0 / 0
2	0.018 / 0.061	0 / 0	0 / 0
7	0.023 / 0.047	0.005 / 0.018	0.001 / 0.011

Table 4. Soil moisture retrieval from τ-homogeneous and heterogeneous regions, using a six-angle system, and different assumptions of the τ composition.

Source of heterogeneity	Range of source considered	Largest likely effect *(reduced)* (m^3m^{-3})	
		Single angle	Multiple angle
Soil roughness	0.0 – 0.3	0.005	0.021 *(0.014)*
Soil moisture	0.20 m^3m^{-3} spread	0.005	0.017
Open water	0.5% absolute error in area estimation	0.100*	0.013*
Vegetation optical depth	Mixtures between 0.0 and 0.6	0.002	0.061 (0.011)

* for scene 50% covered by water

Table 5. Comparison of the effects of different error sources, including for some sources the errors reduced by the methods suggested in each section.

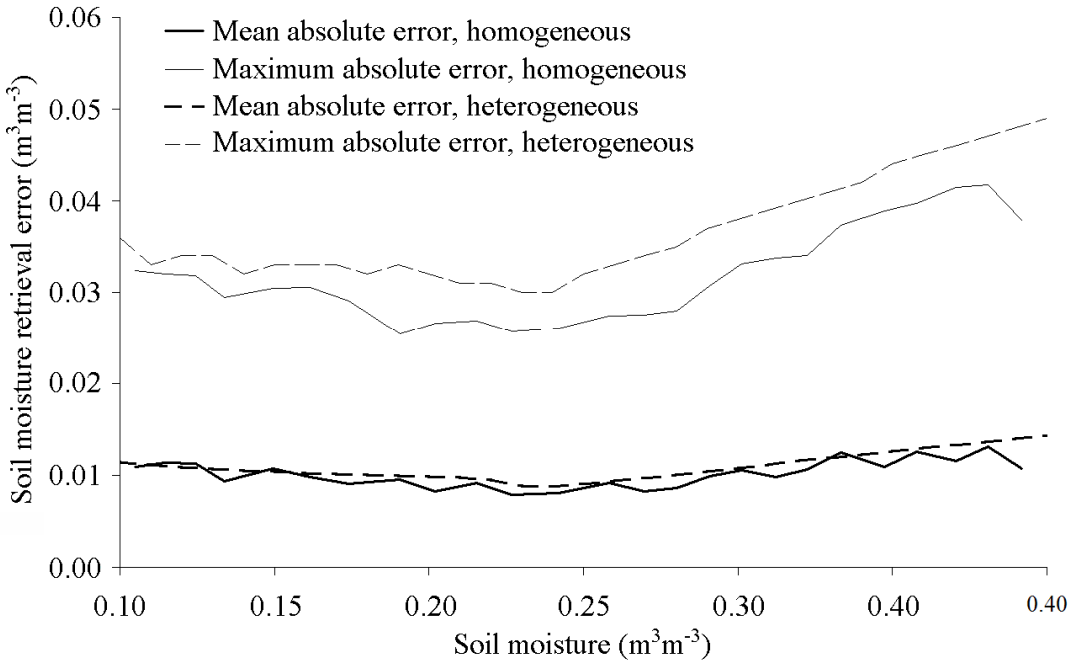

Figure 1. The variation in soil moisture retrieval error caused by a range of soil roughness and retrieving assuming the mean value, as a function of soil moisture for the single-angle system, compared to retrievals for the homogeneous equivalents.

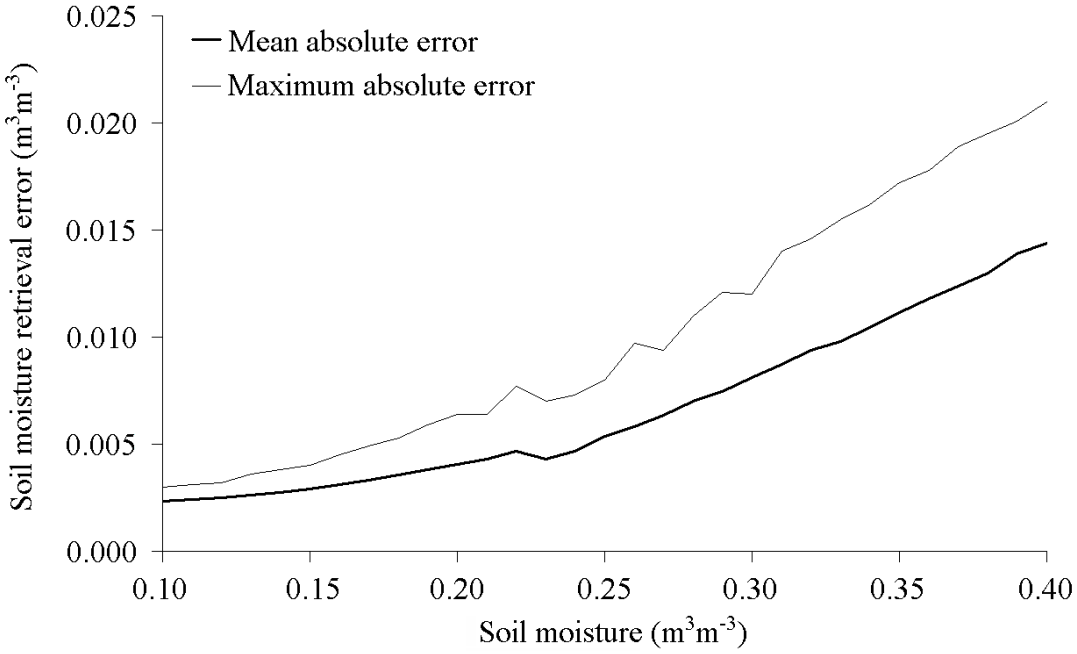

Figure 2. The variation in soil moisture retrieval error caused by a range of soil roughness, as a function of soil moisture for the six-angle system, assuming the average value of surface roughness.

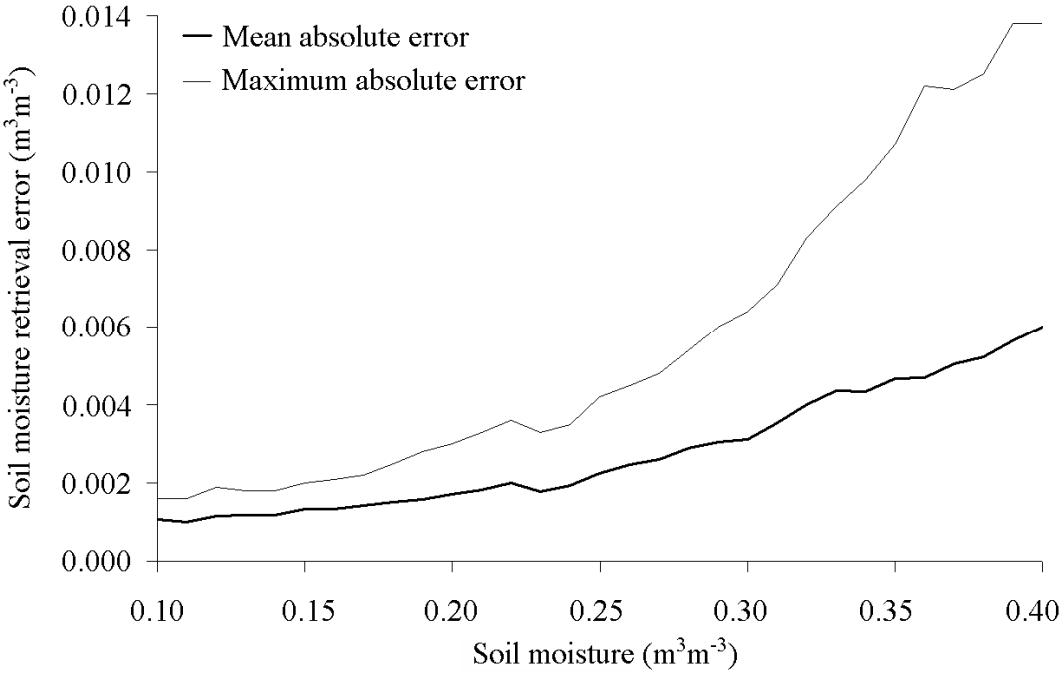

Figure 3. The variation in soil moisture retrieval error caused by a range of soil roughness, as a function of soil moisture for the six-angle system, retrieving a single value of surface roughness.

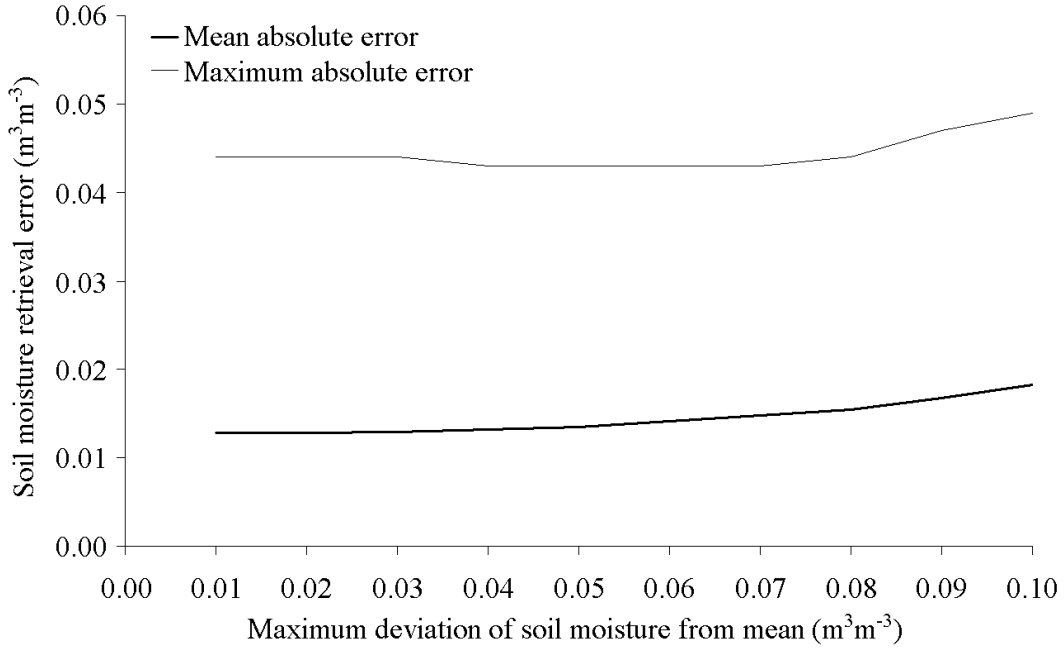

(a) Single-angle retrievals

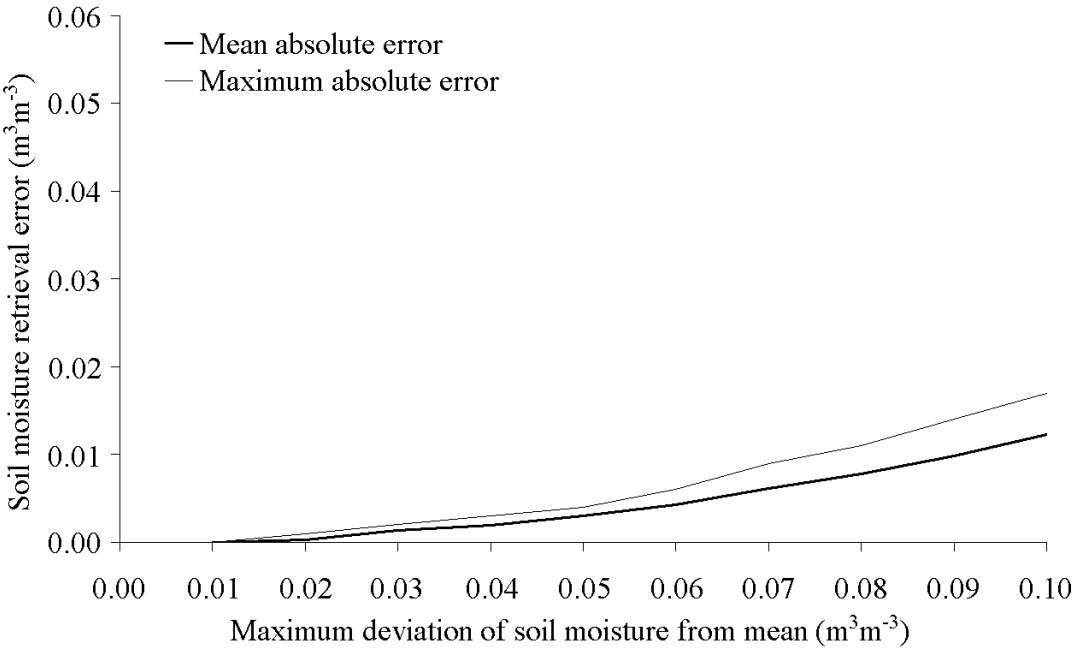

(b) Six-angle retrievals

Figure 4. The effect of soil moisture heterogeneity, statistics over six scenarios.

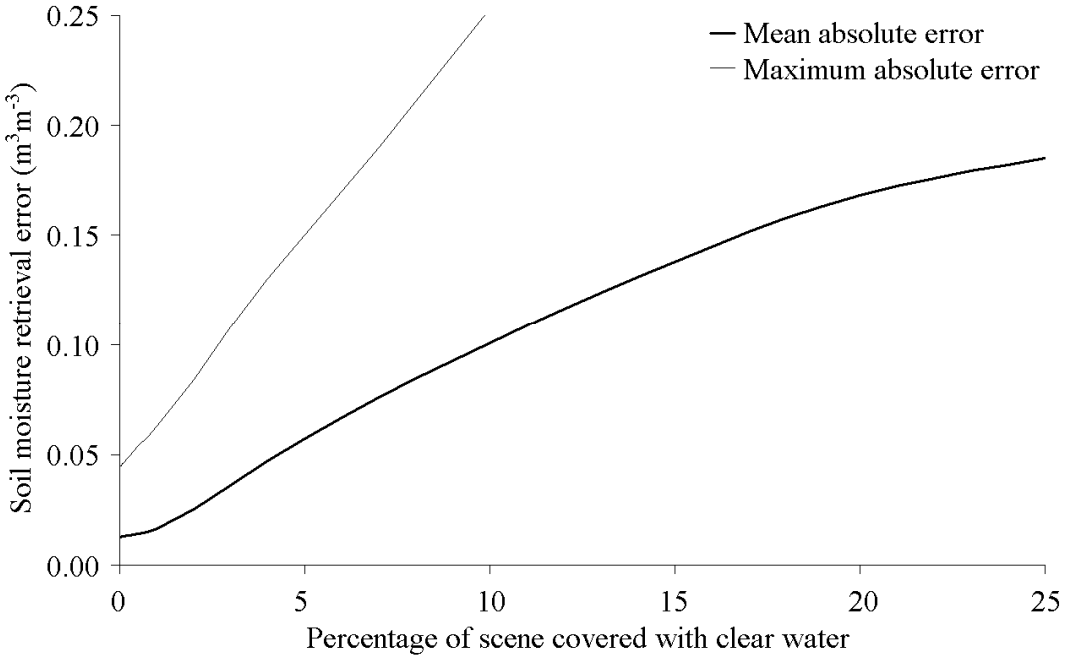

(a) Single-angle retrievals

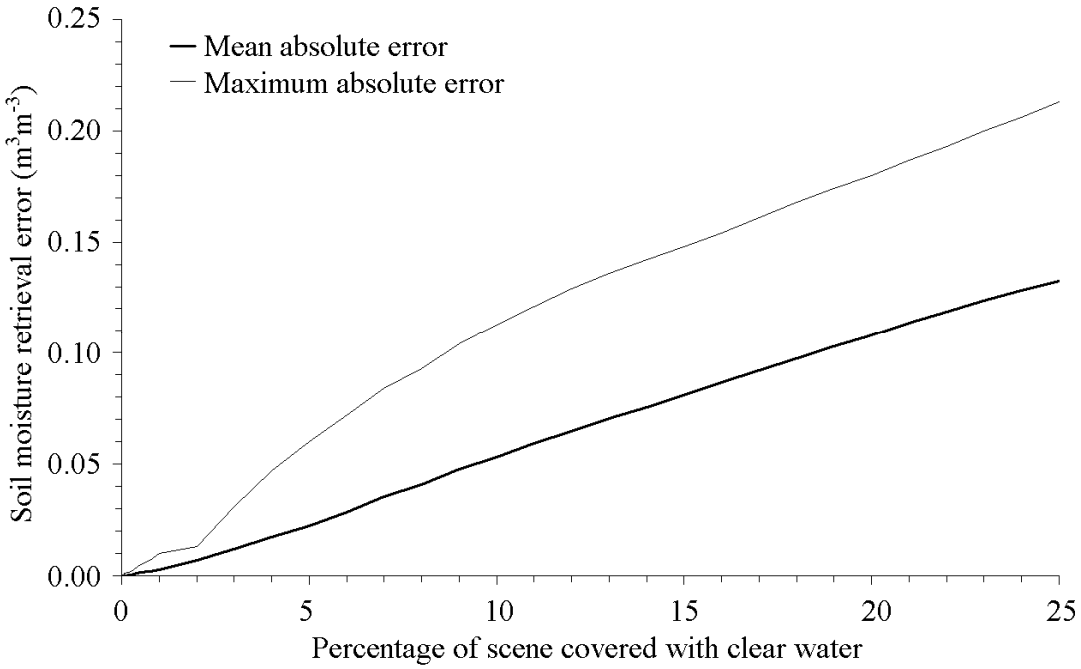

(b) Six-angle retrievals

Figure 5. The effect of water bodies within scene on soil moisture retrieval

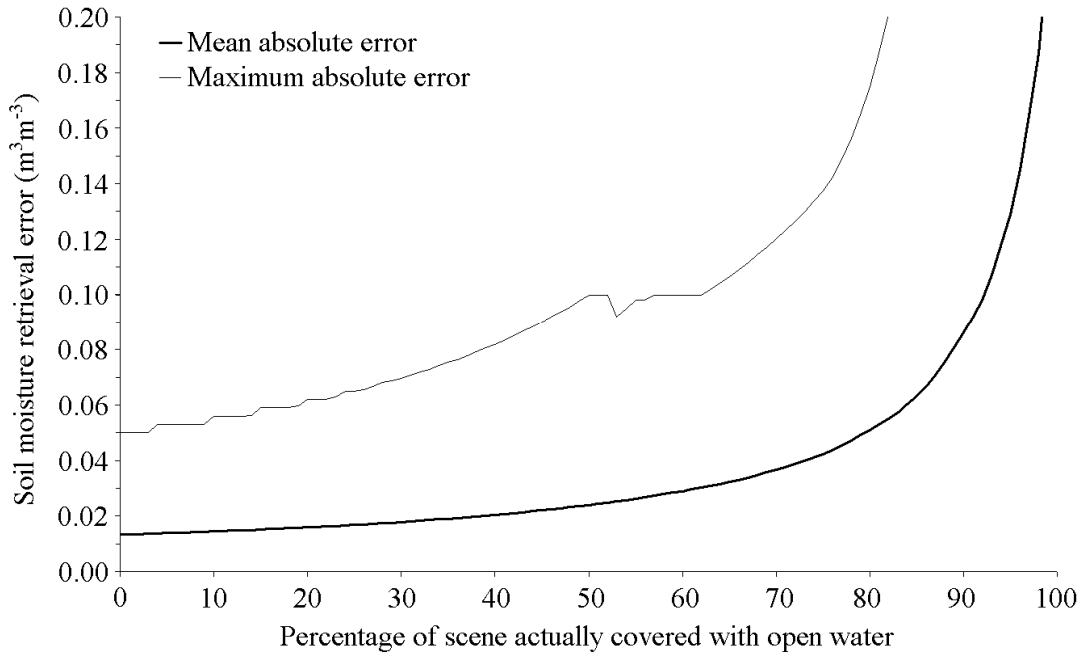

(a)

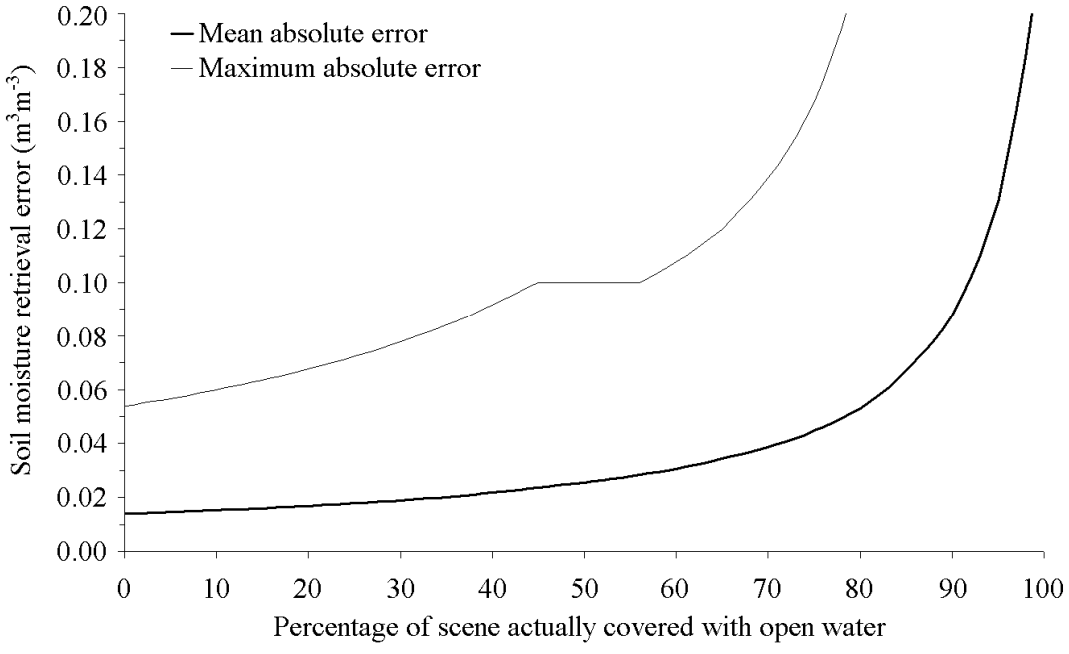

(b)

Figure 6. Soil moisture retrieval error caused by (a) 0.2% and (b) 0.5% errors in estimates of water cover fraction, using a single-angle system.

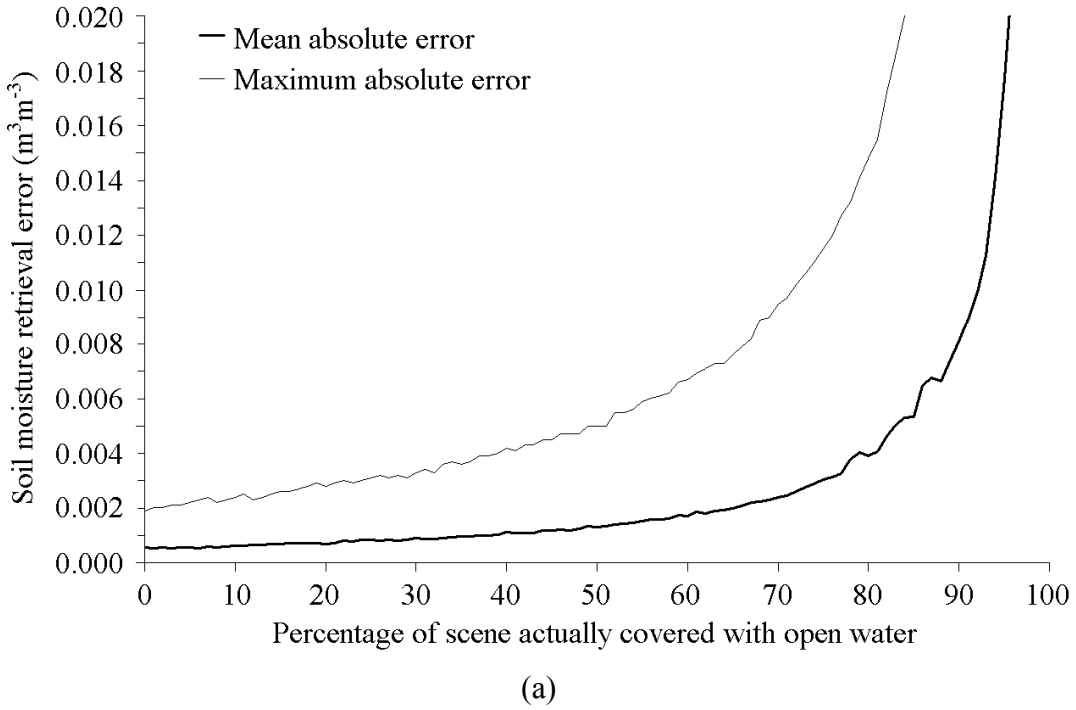

(a)

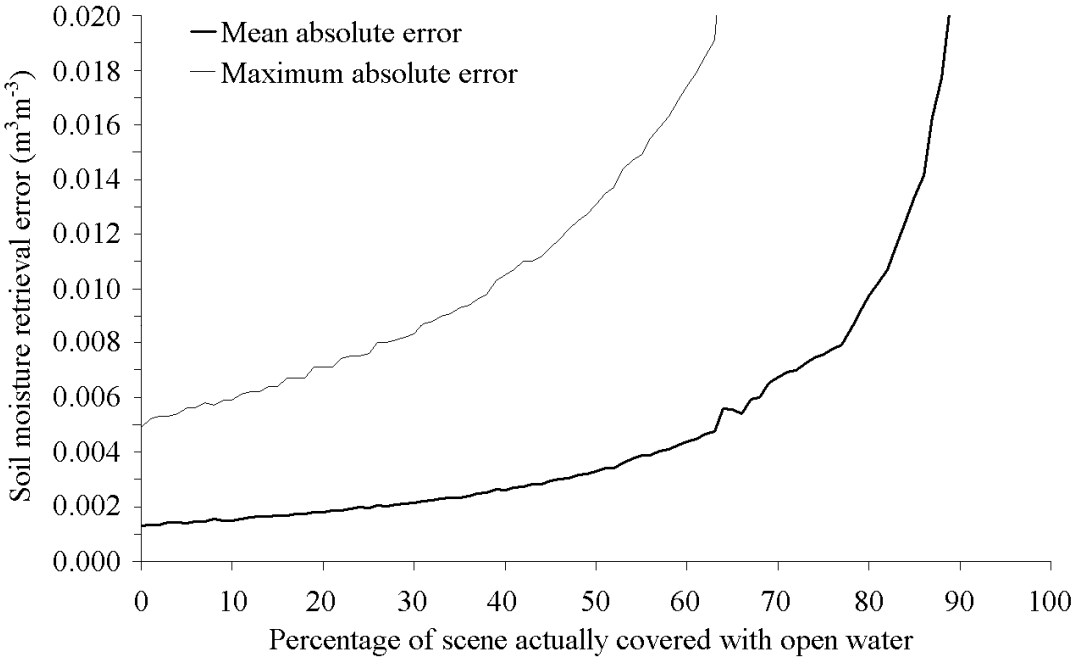

(b)

Figure 7. Soil moisture retrieval error caused by (a) 0.2% and (b) 0.5% errors in estimates of water cover fraction, using a six-angle system.

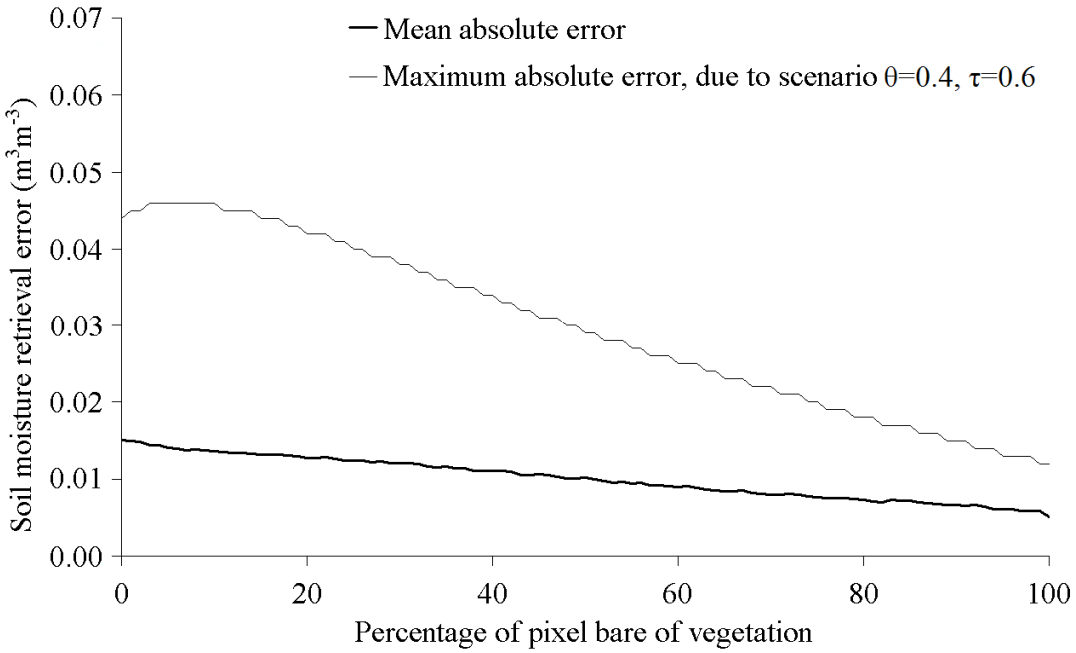

(a) Single-angle retrieval

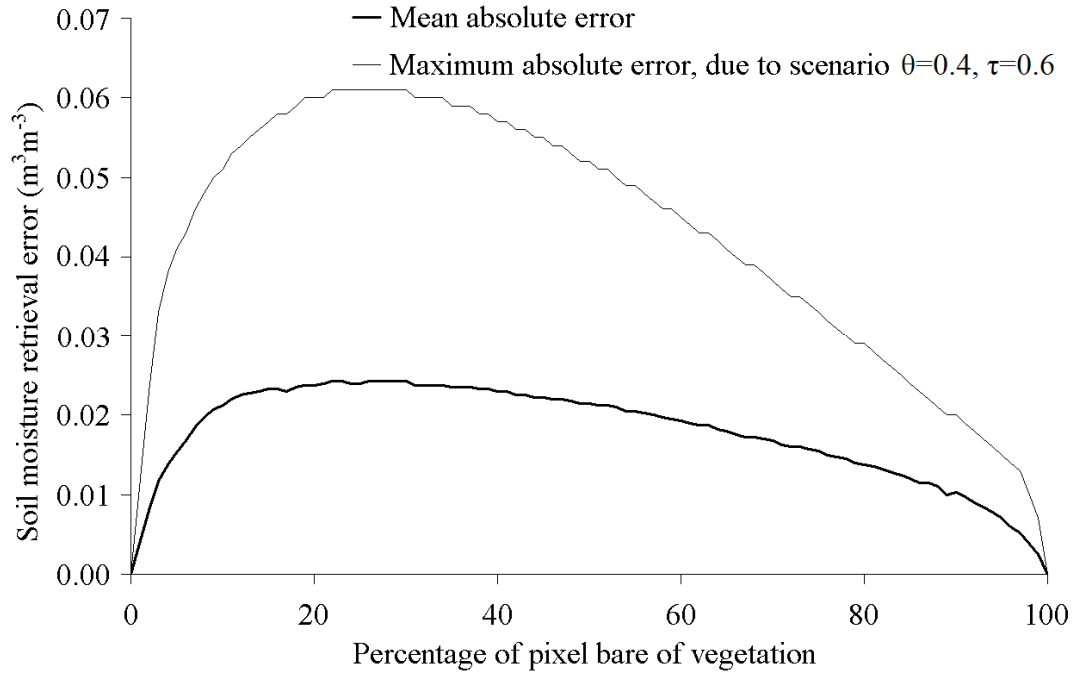

(b) Six-angle retrieval

Figure 8. The error in retrieved soil moisture for a pixel which is a mixture of vegetation-covered and bare soil, using a retrieval which assumes a single value of vegetation optical depth.